FEBS Letters 588 (2014) 4008–4017

journal homepage: www.FEBSLetters.org

Cyclin D1 acts as a barrier to pluripotent reprogramming by promoting neural progenitor fate commitment

Chih-Lung Chen [a,b], Liang-Jie Wang [b], Yu-Ting Yan [c], Hung-Wei Hsu [d], Hong-Lin Su [e], Fang-Pei Chang [a], Patrick C.H. Hsieh [c], Shiaw-Min Hwang [f], Chia-Ning Shen [a,b,d,*]

[a] Graduate Institute of Life Science, National Defense Medical Center, Taipei 114, Taiwan
[b] Genomics Research Center, Academic Sinica, Taipei 115, Taiwan
[c] Institute of Biomedical Sciences, Academic Sinica, Taipei 115, Taiwan
[d] Department of Biotechnology and Laboratory Science in Medicine, National Yang-Ming University, Taipei 112, Taiwan
[e] Department of Life Sciences, National Chung-Hsing University, Taichung 402, Taiwan
[f] Bioresource Collection and Research Center, Food Industry Research and Development Institute, Hsinchu 300, Taiwan

ARTICLE INFO

Article history:
Received 9 June 2014
Revised 11 August 2014
Accepted 27 August 2014
Available online 26 September 2014

Edited by Ned Mantei

Keywords:
Induced pluripotent stem cell
Induced neural stem/progenitor cell
Cyclin D
Cell cycle

ABSTRACT

A short G1 phase is a characteristic feature of the cell cycle structure of pluripotent cells, and is reestablished during Yamanaka factor-mediated pluripotent reprogramming. How cell cycle control is adjusted to meet the requirements of pluripotent cell fate commitment during reprogramming is less well understood. Elevated levels of cyclin D1 were initially found to impair pluripotency maintenance. The current work further identified Cyclin D1 to be capable of transcriptionally upregulating *Pax6*, which promoted reprogramming cells to commit to a neural progenitor fate rather than a pluripotent cell fate. These findings explain the importance of reestablishment of G1-phase restriction in pluripotent reprogramming.

1. Introduction

Pluripotent cells in the inner cell mass exhibit a shortened G1 phase and lack G1 checkpoint regulation [1,2], while neural stem/progenitor cells (NPCs) have a tightly regulated and lengthened G1 phase associated with their self-renewal and differentiation status [3–5]. For example, Lange et al., have recently shown that G1 lengthening is critically regulated during the expansion and differentiation of NPCs into neurons, and Artegiani et al., demonstrated that overexpression of cell cycle regulators cdk4 or cyclin D1 can trigger the expansion of NPCs in adult mouse brain [4,6]. Others have shown that cyclin A2 critically regulates the cell cycle of pluripotent embryonic stem (ES) cells [2,7–9], and a shortened G1 phase protects ES cells from external signals that can induce endodermal or neuroectodermal differentiation [10]. These findings suggest that cell cycle state is modulated during the differentiation process in order to meet the requirements of cell fate commitment during development. However, the key regulators that link cell cycle remodeling and cell fate commitment remain to be explored.

Pluripotent reprogramming, achieved by introducing Yamanaka factors (Oct4, Sox2, c-Myc and Klf4) into somatic cells, has been used to study the pathogenesis of inherited genetic diseases and to identify novel drug targets [11–13]. Recent studies have further demonstrated that Yamanaka factor-mediated fibroblast reprogramming can generate not only induced pluripotent stem (iPS) cells, but also cells that possess features of multipotent hematopoietic progenitors [14] or NPCs [15,16]. Previous work by Ruiz et al., has already shown that cell cycle features of ES cells are acquired during pluripotent reprogramming induced by Yamanaka factors [17]. These findings imply that the fate of cells undergoing reprogramming may be tightly associated with cell cycle remodeling. The present study investigated whether regulators involved in reestablishment of cell cycle structures of ES cells or NPCs during Yamanaka factor-mediated reprogramming are also cell fate

Abbreviations: ES cells, embryonic stem cells; iPS cells, induced pluripotent stem cells; NPCs, neural stem/progenitor cells; EGFP, enhanced green fluorescent protein; SSEA, stage specific embryonic antigen

* Corresponding author. Address: Genomics Research Center, Academic Sinica, 128 Academia Road, Section 2, Nankang, Taipei 115, Taiwan. Fax: +886 2 27899587.
E-mail address: cnshen@gate.sinica.edu.tw (C.-N. Shen).

http://dx.doi.org/10.1016/j.febslet.2014.08.039
0014-5793/

determinants. We found that sustained production of cyclin D1, a G1 phase regulator, during reprogramming possibly acts as a barrier to the successful generation of iPS cells by promoting neural progenitor fate commitment through transcriptionally upregulating *Pax6*.

2. Materials and methods

2.1. Generation of Oct4-EGFP-positive iPS cells

Oct4-EGFP-positive iPS cells were generated as previously described [11,12]. Briefly, for retrovirus packaging and production, pMXs retroviral vectors encoding Oct4, Sox2, Klf4, and c-Myc (obtained from Addgene) were transfected into plat-E cells using polyJet transfection reagents (SignaGen). Passage 1 tail-tip fibroblasts (TTFs) were seeded on 6-well plates at a density of 1×10^5 cells/well for 24 h before retroviral infection. The retrovirus supernatants containing *Oct4*, *Sox2*, *Klf4*, and *c-Myc* were added equally to 6-well plates and incubated for 24 h with 4 μg/ml polybrene. The next day, the virus-containing medium was removed and replaced with fibroblast medium. On day 4, 5×10^4 virus-infected TTFs were seeded on mitomycin C-treated mouse embryonic fibroblast (MEF) feeders and incubated in ES-cell culture medium with leukemia inhibitory factor (LIF) until reprogramming was complete. After 4 passages, the homogenous $EGFP^+$ colonies were picked and evaluated for pluripotency.

2.2. RNA-Seq analysis

RNA was isolated using TRIzol (Invitrogen) according to the manufacturer's instructions. Seven to ten million single-end RNA-Seq reads, of 101 basepairs in length, were generated using an Illumina sequencer and analyzed with CLC Genomics Workbench 4.9 (http://www.clcbio.com). Initially, the reads were trimmed according to quality score and base ambiguity. The processed reads were then mapped to the mouse RefSeq genomic sequences with annotations. The mapped reads of each gene were taken into account to calculate Reads per Kilobase of exon model per Million mapped reads (RPKM), a gene expression measure for RNA-Seq data. For non-specific matches, gene expression was first estimated based on the reads uniquely mapped to the gene, and then used as a weight for the distribution of non-specifically mapped reads. Consequently, 14480 of 34240 predicted genes had at least one mapped read and were detected in more than 3 of 6 samples. R-project was employed to perform the hierarchical clustering of these genes.

Additional methods are described in the Supplementary material.

3. Results and discussion

3.1. Cyclin D1 is induced during cell reprogramming and is co-expressed with neural progenitor markers but not with pluripotency markers

To identify the factors controlling the commitment of reprogramming cells to a pluripotent cell fate, TTFs isolated from 4-week-old mice carrying an Oct4-ΔPE-enhanced green fluorescent protein (Oct4-EGFP) reporter [18] were transduced with retroviruses carrying *Oct4*, *Sox2*, c-*Myc* and *Klf4*. The cells were then cultured on MEF feeders in ES-cell culture medium with LIF. After transduction for 19 days, cell clusters exhibiting a morphology similar to that of ES cells appeared in culture (Fig. 1A). However, very few cell clusters were found to express EGFP. Immunofluorescent staining revealed that the majority of $EGFP^-$ cell clusters were positive for Nestin (Fig. 1B), while $EGFP^+$ cells expressed Nanog (Fig. 1C). To further examine why $EGFP^-$ cells were not reprogrammed into pluripotent cells, the reprogramming cells were divided based on surface expression of EGFP and Stage-Specific Embryonic Antigen-1 (SSEA1) [19]. We distinguished three subpopulations using a FACSAria cell sorter: $EGFP^+/SSEA1^+$ (G^+/S^+), $EGFP^-/SSEA1^+$ (G^-/S^+), and $EGFP^-/SSEA1^-$ (G^-/S^-) (Supplementary Fig. 1A). The G^+/S^+ cell subpopulation was found to display high alkaline phosphatase (AP) activity and features of pluripotent stem cells, including expression of Nanog, SSEA1 and E-cadherin (Supplementary Fig. 1B–E). In contrast, the $EGFP^-$ cell subpopulations (G^-/S^+ and G^-/S^-) did not express EGFP or Nanog, although low levels of AP activity were present. RNA-seq analysis was performed on these three subpopulations together with TTFs, mouse TT2-ES cells, and mouse iPS cells (derived from 30 passages of G^+/S^+ cells in continuous culture). Hierarchical clustering analysis and RT-PCR analysis confirmed that a panel of pluripotency genes including *Nanog* and *Gdf3* were up-regulated in the G^+/S^+ cell population (Fig. 1D and E, Supplementary Fig. 2A and B). Both G^-/S^+ and G^-/S^- cell subpopulations expressed higher levels of *Ccnd1* (cyclinD1) together with some neural genes including *Pax6* and *Nestin*. Ingenuity Pathway Analysis (IPA) revealed that these neural genes are involved either in regulating the self-renewal of NPCs or in development of the central nervous system (Fig. 1D and E, Supplementary Fig. 2A–C). Immunofluorescent staining further confirmed that the majority of cyclin $D1^{hi}/EGFP^-$ cell clusters was positive for Nestin and Sox1 (Fig. 1F and G). These results suggest that reprogramming cells in the G^+/S^+ subpopulation were becoming pluripotent cells, while a large proportion of cyclin $D1^{hi}$ cells in the G^-/S^+ and G^-/S^- subpopulations were committed to neural progenitor fates.

3.2. Subpopulations of reprogramming cells exhibit distinct cell cycle structure

To explore the regulators that link cell cycle remodeling and cell fate commitment during Yamanaka factor-mediated fibroblast reprogramming, the expression patterns of cell-cycle regulators were examined in the different reprogramming cell populations after transduction with Yamanaka factors for 17 days. Immunofluorescent staining showed that $EGFP^-$ cell clusters that expressed Pax6 also displayed higher levels of Cdk6. In contrast, $EGFP^+$ cell clusters that were positive for Nanog expressed low levels of Cdk6 (Fig. 2A and B, arrowed cells). Western blot analysis further confirmed that cyclins A, B1, and H, as well as Cdk1 and Cdk7, were highly expressed in $EGFP^+$ cell subpopulations and in ES cells, while $EGFP^-$ cell subpopulations expressed high levels of cyclin D1, D2, and D3, and Cdk6 (Fig. 2C). We then investigated the percentage of cells in each phase of the cell-cycle using DAPI staining together with 5-ethynyl-2′-deoxyuridine (EdU) labeling (Fig. 2D). In contrast to TTFs, which have the majority of cells in G0/G1 phase, G^+/S^+ cells possessed cell-cycle characteristics similar to those of ES cells, with the majority of cells in S phase. The majority of G^-/S^- and G^-/S^+ cells were in G0/G1 phase.

KEGG mapping applied to the data obtained from RNA-seq analysis confirmed differences in the expression patterns of cell-cycle regulators among TTFs, G^-/S^-, G^-/S^+,G^+/S^+, iPS and ES cells (Supplementary Fig. 3A). G^+/S^+ cells expressed higher levels of S and G2/M phase regulators including *Ccne1*, *Ccna2* and *Ccnb1* (which are known to promote entry into S and G2/M phases, Supplementary Fig. 3C and D), while $EGFP^-$ cell subpopulations (G^-/S^- and G^-/S^+) expressed higher levels of G1 phase regulators including *Ccnd1*, *Cdk6*, *Cdkn1a*, and *Cdkn1b* (which are known to form kinase complexes regulating entry into G1 phase, Supplementary Fig. 3B). Further characterization showed that the majority of cyclin $D1^{hi}/EGFP^-$ cells were associated with expression of a panel of neural

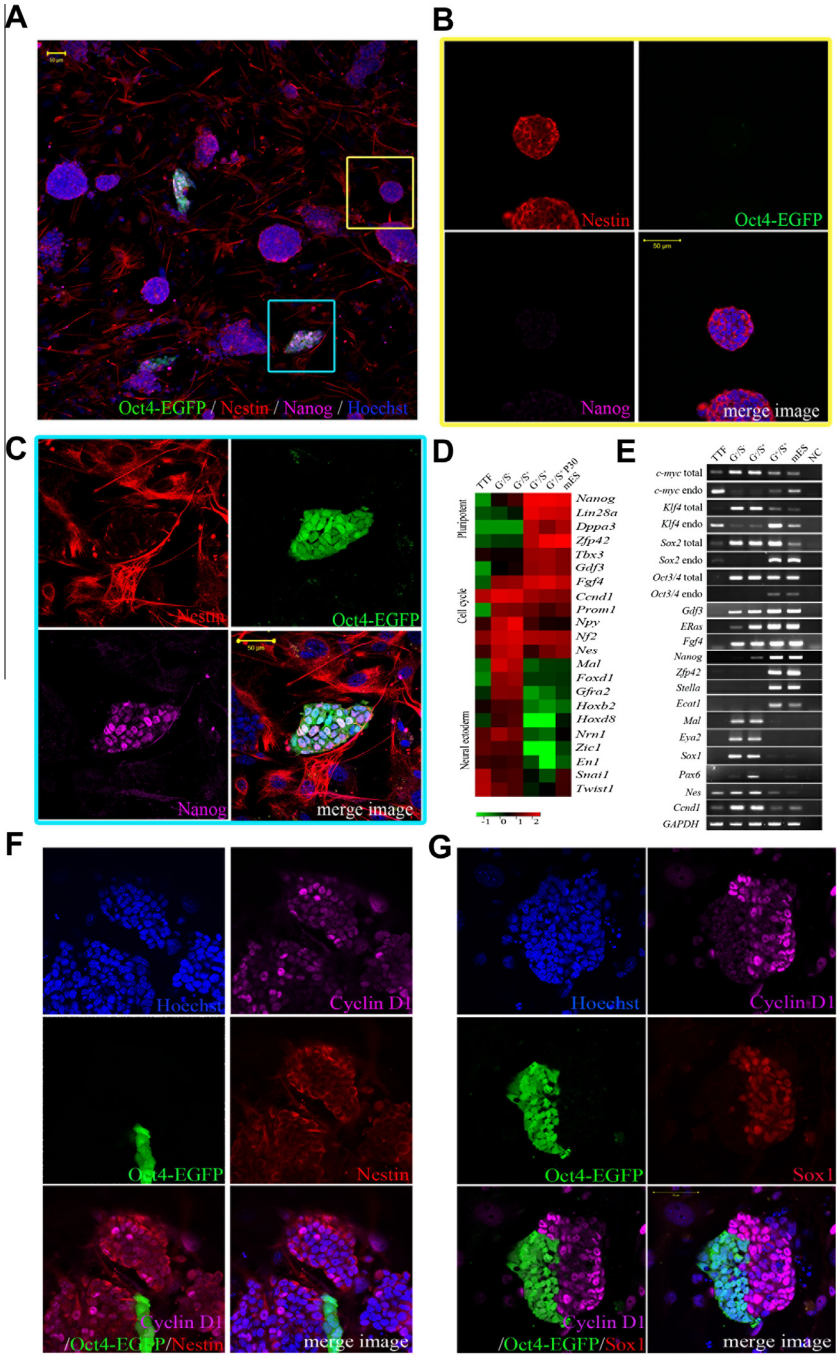

Fig. 1. Cyclin D1 is induced during cell reprogramming and is co-expressed with neural progenitor markers but not with pluripotency markers. TTFs isolated from 4-week-old mice carrying an Oct4-EGFP reporter were transduced with retroviruses carrying *Oct4*, *Sox2*, c-*Myc* and *Klf4*. (A–C) The reprogramming cells at day 19 were fixed and stained with anti-Nanog (purple) and anti-Nestin (red) antibodies. Cell nuclei were counterstained with Hoechst dye (blue) and EGFP is in green. Only the EGFP-positive cells also express Nanog. Scale bar represents 50 μm. (D and E) The reprogramming cells were divided into three subpopulations: G^+/S^+, G^-/S^+, and G^-/S^- based on surface expression of EGFP (G) and SSEA1 (S) analyzed using a FACSAria cell sorter. (D) Hierarchical clustering analysis of gene expression patterns of TTF (passage 2), G^-/S^- (passage 5), G^-/S^+ (passage 5), G^+/S^+ (passage 5), G^+/S^+ (passage 30), and ES cells. The Reads per Kilobase of exon per Million mapped reads (RPKM) of RNA sequences determined as described in the Section 2 were taken log2 and the hierarchical clusters were determined using the hclust method of R-project. Only genes with more than a twofold difference between any pair of samples from different classes are shown in the heat map. The pluripotent, neural stem/progenitor, and cell cycle regulators were isolated for hierarchical clustering analysis. (E) Total RNA was extracted from TTF (passage 2), G^-/S^- (passage 5), G^-/S^+ (passage 5), G^+/S^+ (passage 5), and ES cells. The selected genes in control and experimental groups were analyzed by RT-PCR with specific primers. For reprogramming genes, "endo" refers to PCR with primers specific for the endogenous gene, and "total" to PCR with primers detecting expression of both the endogenous and retrovirally encoded genes. (F and G) The reprogramming cells at day 17 were fixed and stained with anti-Nestin (red), anti-Sox1 (red) and anti-cyclin D1 (purple) antibodies. EGFP is in green. Cell nuclei were counterstained with Hoechst dye (blue). Scale bar represents 50 μm.

genes that included *Nestin*, *Sox3*, *Tau*, *Zic2 and Sox1* (Supplementary Fig. 4) and high levels of cyclin D1 were correlated with expression of Pax6 (Supplementary Fig. 5A and B). In contrast, cyclin D1 levels were negatively correlated with Nanog and Oct4-EGFP expression (Supplementary Fig. 5C–F).

Noticeably, we found that $EGFP^-$ cells grew slower and had longer doubling time (18 h) than did $EGFP^+$ cells (12 h). To further determine if the higher proportion of $EGFP^-$ cell in G0/G1 phase was due to increases in length of G1 phase in comparison to $EGFP^+$ cells, $EGFP^+$ and $EGFP^-$ cells were synchronized in mitotic phase by

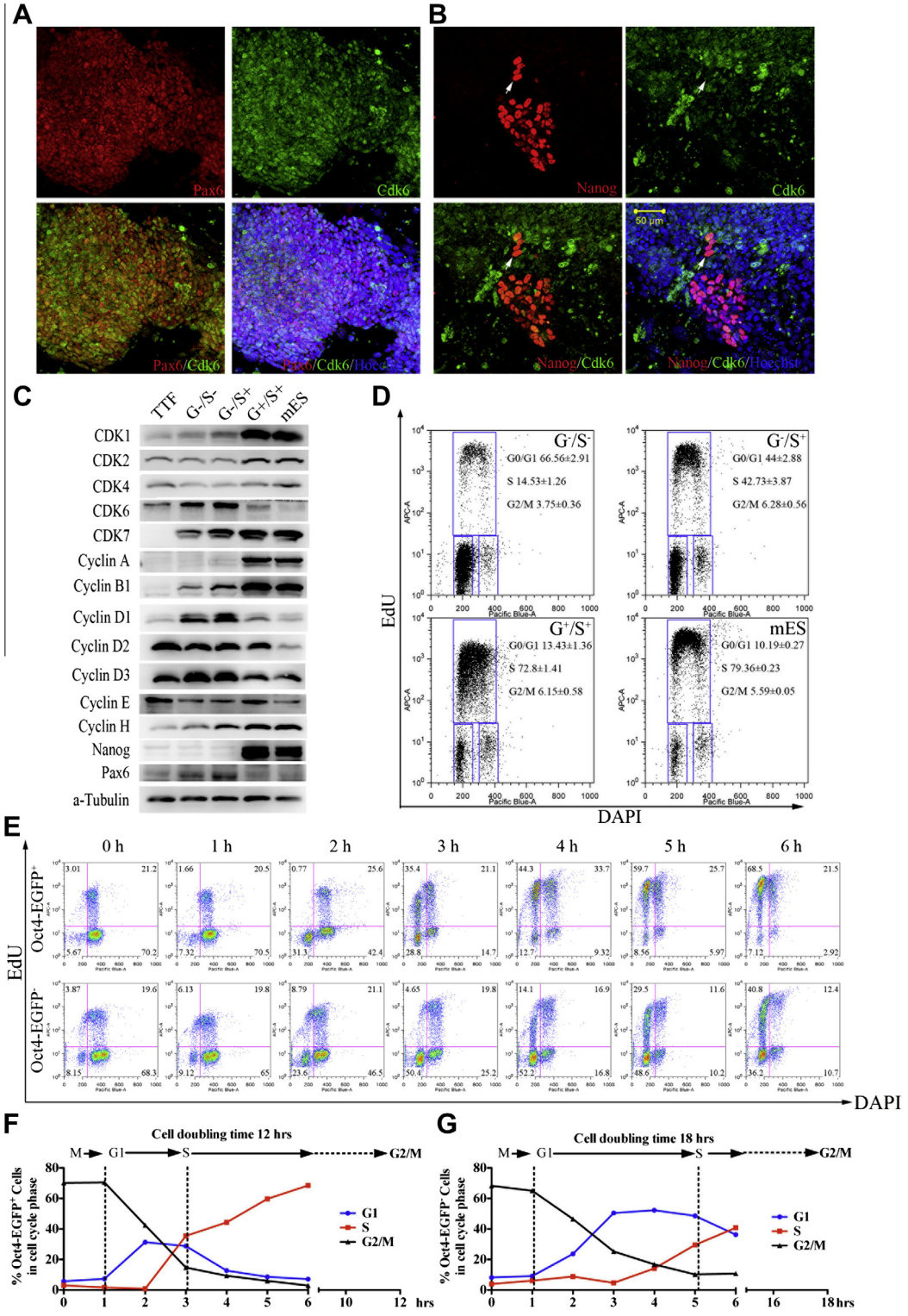

Fig. 2. Subpopulations of reprogramming cells exhibit distinct cell cycle properties. (A and B) Day 17 reprogramming cells were fixed and stained with anti-Pax6 (red), anti-Nanog (red), and anti-CDK6 (green) antibodies. Cell nuclei were counterstained with Hoechst dye (blue). Scale bar represents 50 μm. (C) Total proteins were isolated from TTFs (passage 3), G^-/S^- (passage 5–6), G^-/S^+ (passage 5–6), G^+/S^+ (passage 5–6), and ES cells for Western blot analysis, and 20 μg total protein were loaded for antibody detection; α-tubulin was used as an internal control. (D) Subpopulations of reprogramming cells were labeled with EdU (10 μM for 45 min) and fixed. Incorporation of EdU was detected with azide-conjugated Alexa649 and cells were incubated with DAPI for chromosome staining. The cells were analyzed with FACSCanto. (E–G) Synchronization of Oct4-EGFP$^+$ and Oct4-EGFP$^-$ cells with colcemid (40 ng/ml for 7 h) followed by their release from the mitotic arrest. The cells were labeled with EdU after removing the colcemid and were isolated at different time points and fixed with 4% PFA. The percentages of G0/G1, S, and G2/M phase of the cell cycle were analyzed by FACSCanto cytometry based on EdU and DAPI signal intensity.

Colcemid treatment for 7 h (Fig. 2E–G) [20]. Between 1 and 2 h after their release from the mitotic arrest, both EGFP$^+$ and EGFP$^-$ cells had undergone transition from M-to-G1 phase (Fig. 2F and G). EGFP$^+$ cells were found to have a rapid transition from G1-to-S phase, between 2 and 4 h, in comparison to EGFP$^-$ cells where the G1-to-S phase transition occurred after 5 h (Fig. 2F and G). Taken together, these findings indicate that, in comparison to EGFP$^+$ cells, cyclin D1^{hi}/EGFP$^-$ cells exhibit a lengthened G1 phase and display NPC-like characteristics.

3.3. Elevated levels of cyclin D1 impair pluripotency maintenance and promote neural differentiation

EGFP$^+$ cells possessed several pluripotency features including (i) absence of CpG methylation in the *Nanog* promoter region (Fig. 3A), (ii) were positive for Nanog expression (Fig. 3B), and (iii) had the capability to differentiate into cells of the three germ layers in vivo and in vitro (Fig. 3C–E). Pluripotent ES cells exhibit an unusual cell-cycle that has a lengthened S phase and a very short G1 phase [7,21,22]. We reasoned that evaluated level of cyclin D1 may affect pluripotency maintenance. We therefore next examined if overexpression of Cyclin D1 affects pluripotency characteristics of EGFP$^+$ cells. To address this question, cyclin D1 was overexpressed (Fig. 3F–H) in G$^+$/S$^+$ cells at passage 1 and FACS-purified cells were continuously passaged 4 times on MEF feeders in LIF-containing medium before being analyzed by immunofluorescent staining and flow cytometry. As shown in Fig. 3F and G, overexpression of cyclin D1 led to a 72% reduction in the number of EGFP$^+$ cells. RT-PCR analysis further confirmed that the reduction in EGFP$^+$ cells was accompanied by decreased expression of a panel of pluripotency genes that included *Oct4*, *Sox2*, *c-Myc*, *Klf4*, *Cripto*, *Gdf3*, *n-Myc*, *Nanog*, *SOCS3* and *Dppa3* (Fig. 3H). We addressed the issue further by overexpressing cyclin D1 in iPS cells (Fig. 3I and J) and in ES cells (Fig. 3K–N), and observed the appearance of Nestin-expressing colonies composed of cells displaying an elongated cell morphology (Fig. 3N) accompanied by loss of EGFP (Fig. 3J, arrowed cells) or Nanog expression (Fig. 3M, arrowed cells). EB formation and teratoma formation experiments showed that overexpression of cyclin D1 promoted the differentiation of iPS and ES cells into neural lineages (Supplementary Fig. 6A–C, G–J and M–O).

3.4. Cyclin D1 regulates neural progenitor fate commitment during Yamanaka factor-mediated fibroblast reprogramming

To further investigate how cyclin D1^{hi}/EGFP$^-$ cells become committed to an NPC-like cell fate during reprogramming, day 9 EGFP$^-$ cells were collected and seeded on poly-L-lysin/laminin-coated glass coverslips in NPC growth medium. The cells were found to express cyclin D1 and NPC markers including Sox1, Nestin, Pax6 and CD133 (Fig. 4A–C. Supplementary Fig. 7A–D), and were able to form neurospheres and to be continuously passaged more than 10 times without losing their growth capacity (Supplementary Fig. 7E). Replacing the NPC growth medium with serum-containing medium could trigger sphere cells to differentiate into Tuj1$^+$ neurons, GFAP$^+$ glial cells and O4$^+$ oligodendrocyte precursor cells (Fig. 4D–F). Since RT-PCR and FACS analysis (Supplementary Fig. 4D–G) showed that cyclin D1 was up-regulated by transduction with Yamanaka factors and was associated with increased expression of NPC genes, we investigated whether cyclin D1 is involved in regulating the generation of NPC-like cells during reprogramming. TTFs were transduced with Yamanaka factors and subjected to shRNA-mediated *Ccnd1* knockdown (70% knockdown efficiency, Supplementary Fig. 8A and D). After 14 days in culture, a significant reduction in the number of total colonies (reduced by 39%) and of Pax6-positive cell clusters (reduced by 39%) was observed, and was accompanied by a reduced proliferation rate and decreased expression of *Sox3*, *Pax6* and *Gfap* (Fig. 4G–I; Supplementary Fig. 8A–E). Additionally, an increased proportion of reprogramming cells was observed to differentiate into Tuj1$^+$ (β3-tubulin-expressing) neuronal cells (Supplementary Fig. 8B and E). Indeed, Cyclin D1 is known to be involved in regulating the self-renewal expansion of NPCs [4], and reduction of cyclin D1 can promote differentiation of NPCs to neuron. The results suggest that *Ccnd1* knockdown possibly affects maintenance of reprogramming cell-derived NPCs and progenitor cell fate.

Importantly, cyclin D1 was found to negatively modulate the generation of iPS cell precursors at an early reprogramming stage, as Nanog-expressing colonies were found to increase by 220% (Fig. 4J). RT-PCR analysis further confirmed that the increase in Nanog-expressing cells was accompanied by up-regulation of a panel of pluripotent genes including *Cripto*, *Gdf3*, *n-Myc*, *Dppa3 and Nanog* (Fig. 4K). Cyclin D1 was further knocked down in G$^+$/S$^+$ cells at passage 1, and FACS-purified cells were continuously passaged 4 times on MEF feeders in LIF-containing medium before being analyzed by immunofluorescent staining and flow cytometry. As shown in Fig. 4L, cyclin D knockdown led to a 124% increase in the number of EGFP$^+$ cells. The shRNA-mediated *Ccnd1* knockdown was further carried out in iPS and R1-ES cells. This did not affect the expression of pluripotency markers (data not shown), but in vitro differentiation experiments showed that *Ccnd1* knockdown reduced the capability of ES and iPS cells to differentiate into neural lineages (Supplementary Fig. 6D–F, K and L). The findings suggest that a reduction in cyclin D1 would be beneficial for pluripotency maintenance.

3.5. Cyclin D1 promotes neural progenitor fate commitment and suppresses pluripotent reprogramming via transcriptionally modulating expression levels of Pax6 and Nanog

To further explore how elevated levels of cyclin D1 can promote the commitment of reprogramming cells to a neural progenitor fate, we analyzed the binding sites of transcriptional factors in the *Pax6* promoter region using PROMO 3.0 [23], and found that the Yamanaka factors Oct4, Sox2, Klf4, and c-Myc can potentially bind to a 2 kb region of the *Pax6* promoter. To examine whether cyclin D1 transcriptionally regulates *Pax6* expression, we prepared a luciferase reporter construct containing 2 kb of the *Pax6* promoter region (Fig. 5A). Moreover, using a genetic-proteomic screen, Bienvenu et al., previously demonstrated that cyclin D1 affects transcription during development [24]. According to data obtained from chromatin immunoprecipitation experiments, cyclin D1 can bind via interaction with NF-Y to the −100 to −200 bp region of the *Pax6* promoter in retinal cells. Using a co-immunoprecipitation assay, we initially validated that cyclin D1 can form a complex with NF-Y in reprogramming cells (Fig. 5B). We then further showed that overexpression of cyclin D1 or cyclin D1 T286A mutant (less degradable form) [25] increased *Pax6* promoter activity (Fig. 5C). In contrast, constitutive expression of kinase-dead mutant, cyclin D1-K112E, suppressed *Pax6* promoter activity (Fig. 5C) [26]. The results imply that cyclin D1 is able to transcriptionally regulate *Pax6* expression in reprogramming cells.

Pax6 is a transcriptional determinant of the neuroectodermal fate during development [27]. In order to evaluate whether expression of Pax6 critically regulates the commitment of reprogramming cells to NPCs, TTFs were transduced with Yamanaka factors with or without overexpression of Pax6. After transduction for 17 days, expression of Nanog and Nestin was examined using immunofluorescent staining. The majority of reprogramming cells expressed Nestin (Fig. 5D–F). The number of EGFP$^+$ and Nanog$^+$ colonies was reduced by 93% and 90% (Fig. 5G and H), respectively, accompanied by down-regulation of a panel of pluripotent genes

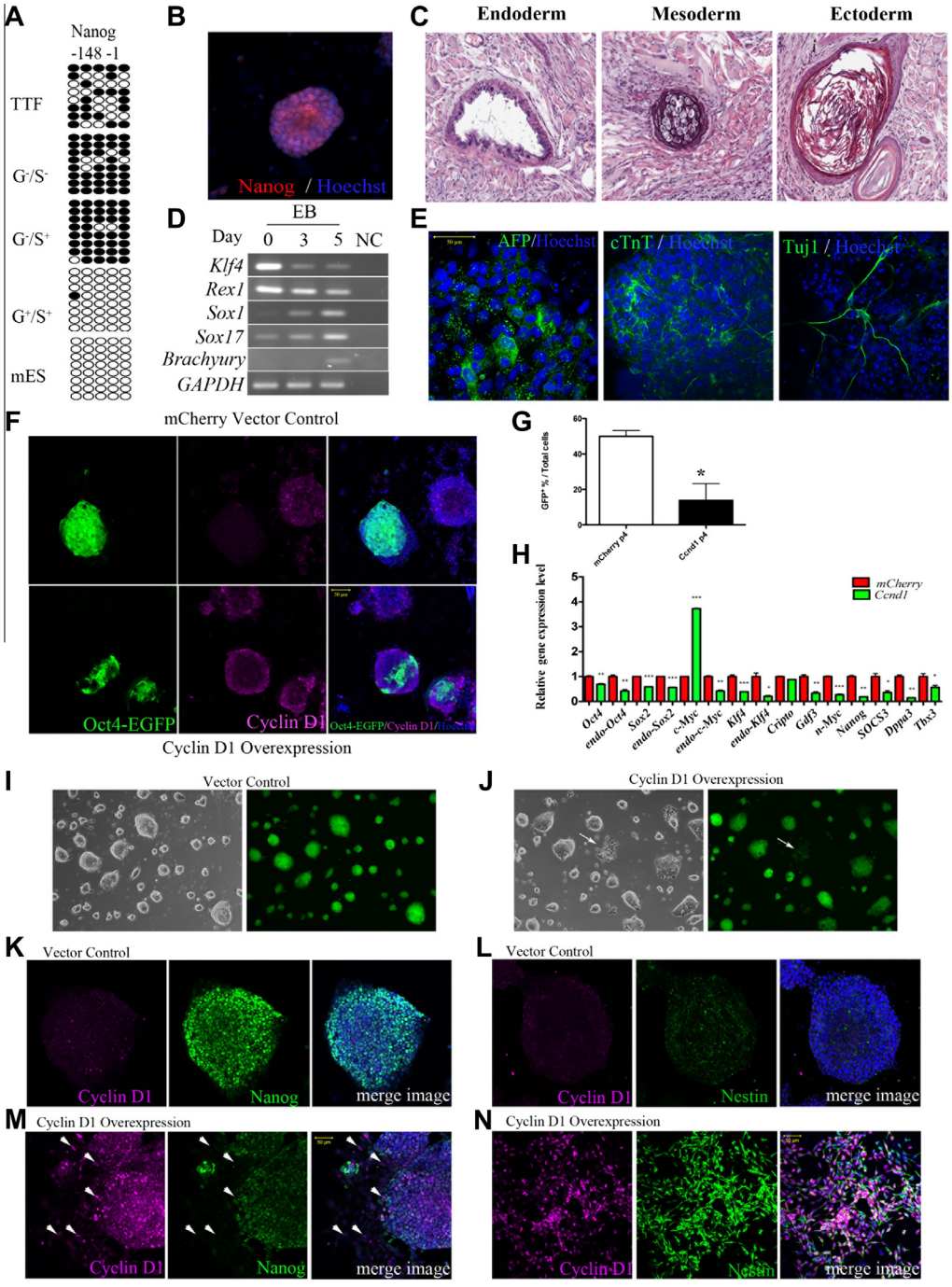

Fig. 3. Constitutive expression of *Ccnd1* in Oct4-EGFP$^+$ cells impairs pluripotency maintenance. (A) Genomic DNA isolated from TTF, G$^-$/S$^-$ (passage 5), G$^-$/S$^+$ (passage 5), G$^+$/S$^+$ (passage 5), and mES cells was used for bisulfite sequencing. Black ovals indicate the presence and white ovals the absence of methyl-CpG at positions in the region analyzed. (B) G$^+$/S$^+$ cells at passage 5 were fixed and stained with anti-Nanog (red) antibodies. Cell nuclei were counterstained with Hoechst dye (blue). (C) 1×10^6 G$^+$/S$^+$ cells were subcutaneously injected into NOD/SCID mice, which were analyzed for formation of teratomas after 1 month. (D) 1×10^6 G$^+$/S$^+$ cells were plated on 6 cm petri dishes with 5 ml mES culture medium without LIF. The G$^+$/S$^+$ cells and embryoid bodies were collected at days 0, 3, and 5. RT-PCR analysis was performed to determine the expression of pluripotency markers *Klf4* and *Rex1*, ectodermal marker *Sox1*, mesodermal marker *Brachyury*(*T*), and endodermal marker *Sox17*. (E) 3-Day embryoid bodies were seeded on culture dishes in culture medium without LIF and were grown for 5 days. Attached cells were then fixed and stained with anti-AFP (hepatocytes, endoderm), anti-cTnT (cardiomyocytes, mesoderm) and Tuj1 (neurons, ectoderm) antibodies. Cell nuclei were counterstained with Hoechst dye (blue). (F–H) Day 17 reprogramming cells were transfected with pLKO.1-EF1-IRES-mCherry (vector control) or pLKO.1-EF1-cyclin D1-IRES-mCherry. After 48 h, cells that were EGFP$^+$ and mCherry$^+$ were purified using a FACSAria cell sorter and then cultured on MEF feeders. The reprogramming cells at passage 4 were fixed and stained with anti-cyclin D1 (purple) antibodies (cell nuclei were counterstained with Hoechst dye (blue) and EGFP is in green (F). The reprogramming cells at passage 4 were analyzed by a FACSAria cell sorter (G) or analyzed by real-time quantitative PCR (H) for *Oct4*, *Sox2*, *c-Myc*, *Klf4*, *Cripto*, *Gdf3*, *n-Myc*, *Nanog*, *SOCS3*, *Dppa3*, and *Tbx3*. Values shown are mean ± S.E.M., $n = 3$. $^*p < 0.05$, $^{**}p < 0.01$, $^{***}p < 0.001$ indicates that the difference between mCherry and *Ccnd1* treatment was statistically significant. Mann–Whitney test was used for determining statistical significance. (I and J) Photos of cell morphologies of control (mCherry vector only) or Cyclin D1-overexpressing iPS cells were taken under bright field or GFP channel. Arrows mark the differentiated cells with weak GFP and neural cell morphology. (K and M) Immunofluorescent staining was performed for cyclin D1 (purple), and Nanog (green) on *mCherry* or *Ccnd1* transgenic ES-R1. The panels labeled "merge image" show these stainings merged with anti-Nanog in green, anti-cyclin D1 in purple, and staining of cell nuclei with Hoechst dye in blue. Arrowheads mark the differentiated cells with weak Nanog. Scale bar represents 50 μm. (L and N) Immunofluorescent staining of cyclin D1 (purple) and Nestin (green) on *mCherry* or *Ccnd1* transgenic ES-R1. The merge image represents an overlay of the anti-Nestin, and anti-cyclin D1 images along with the Hoechst33342 stained images for DNA. Scale bar represents 50 μm.

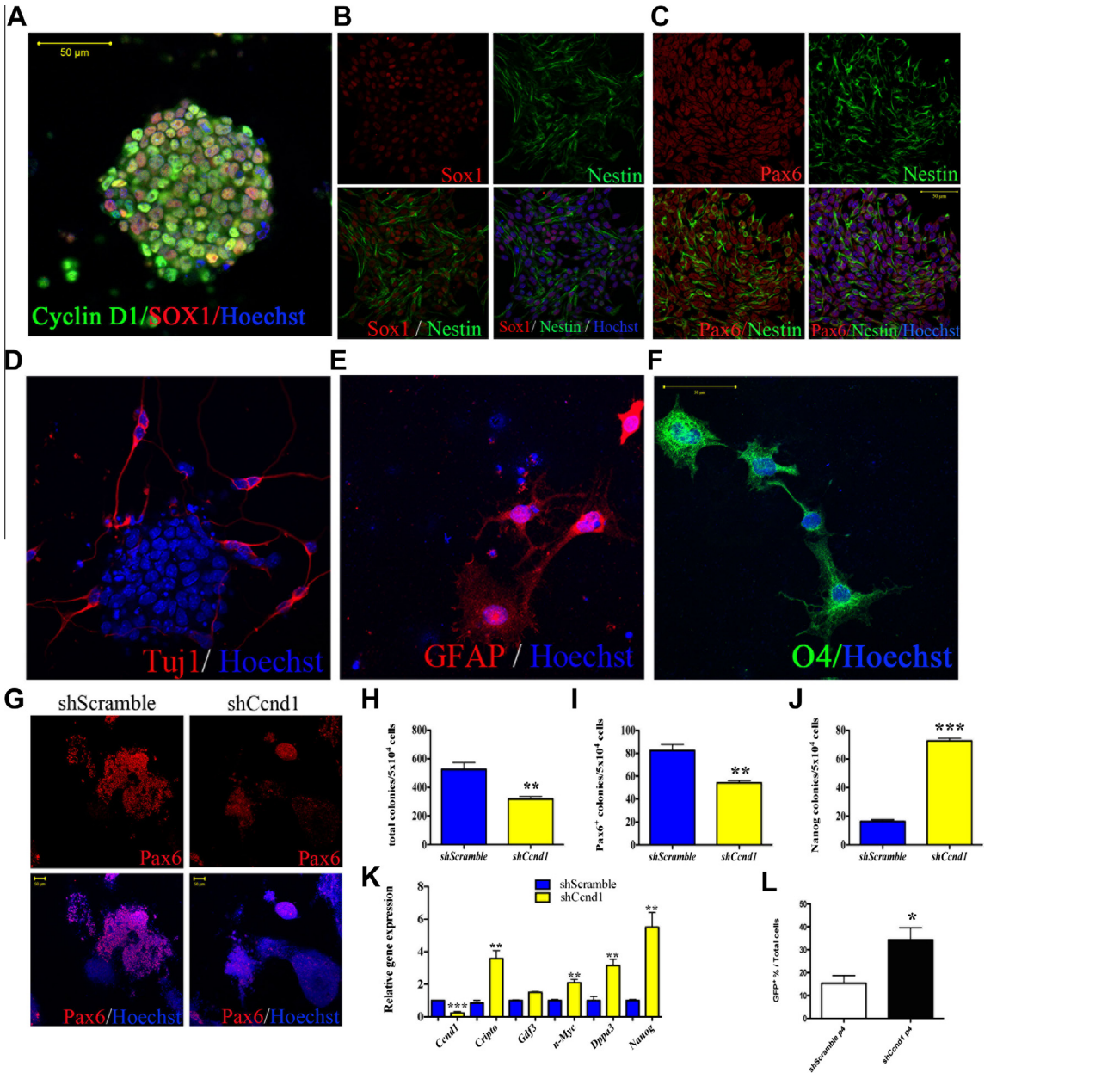

Fig. 4. Cyclin D1 modulates neural progenitor commitment in cell reprogramming, (A–F) Characterization of sphere-forming cells derived from Yamanaka factor-mediated TTF reprogramming. Cyclin D1 expression was found to be highly correlated with Sox1 and Pax6 expression in EGFP$^-$ cells. (A) Day 9 EGFP$^-$ reprogramming cells were grown in neurosphere culture medium for several passages. The sphere cells at passage 8 were fixed and stained with anti-cyclin D1 (green) and anti-Sox1 (red) antibodies. Cell nuclei were counterstained with Hoechst dye (blue). (B and C) The EGFP$^-$ spheres were resuspended as single cells, seeded on poly-L-lysin/laminin coated coverslips, and cultured until 70–80% confluent. Cells were then fixed and stained with anti-Sox1 (red)/anti-Nestin (green) or anti-Pax6 (red)/anti-Nestin (green) antibodies. Cell nuclei were counterstained with Hoechst dye (blue). (D–F) The sphere cells at passage 8 were seeded in either growth factor-withdrawn medium (for neuronal differentiation) or serum-containing medium (for glial and oligodendrocyte differentiation) for 5 days, and then were fixed and stained with anti-Tuj1 (red), anti-GFAP (red) or anti-O4 (green) antibodies. Cell nuclei were counterstained with Hoechst dye (blue). (G–K) Day 3 reprogramming cells were infected with lentivirus carrying *shCcnd1* or *shScramble* and selected with puromycin from day 5 to day 17. Day 17 reprogramming cells were fixed and stained with anti-Pax6 (red) or anti-Nanog antibodies. Cell nuclei were counterstained with Hoechst dye (blue). Total colonies, Pax6$^+$, and Nanog$^+$ colonies derived from reprogramming cells infected with lentivirus carrying *shCcnd1* or *shScramble* were counted under a microscope. Gene expression was analyzed by real-time quantitative PCR (K) for *Ccnd1*, *Cripto*, *Gdf3*, *n-Myc*, *Nanog*, and *Dppa3*. Values shown are mean ± S.E.M., $n = 3$. $^{**}p < 0.01$, $^{***}p < 0.001$ indicate that the differences between *shScramble* and *shCcnd1* treatments were statistically significant. Mann–Whitney test was used for determining statistical significance. Scale bar represents 50 μm. (L) G$^+$/S$^+$ cells at passage 1 were infected with lentivirus carrying *shCcnd1* or *shScramble* and were selected with puromycin for another 3 days. The reprogramming cells at passage 4 were analyzed by a FACSAria cell sorter. Values shown are mean ± S.E.M., $n = 3$. $^*p < 0.05$ indicates that the difference between shScramble and shCcnd1 treatment was statistically significant. Mann–Whitney test was used for determining statistical significance.

including *Cripto*, *Gdf3*, *n-Myc*, and *Nanog* (Fig. 5I). Recently, Zhang et al. showed that overexpression of Pax6a is sufficient to trigger human ES cells to differentiate into neuroectodermal lineages via induction of neural genes [27]. The report further demonstrated that Pax6a or Pax6b could repress pluripotency through direct binding to pluripotency gene promoters. The current findings imply a similar regulatory mechanism may be present in mouse pluripotent cells.

The observation that Nanog expression levels were altered after cyclin D1 overexpression or knockdown in G$^+$/S$^+$, iPS and ES cells (Figs. 3H and M and 4K) led us to question whether, in addition to repression of pluripotency by direct binding of Pax6 to pluripo-

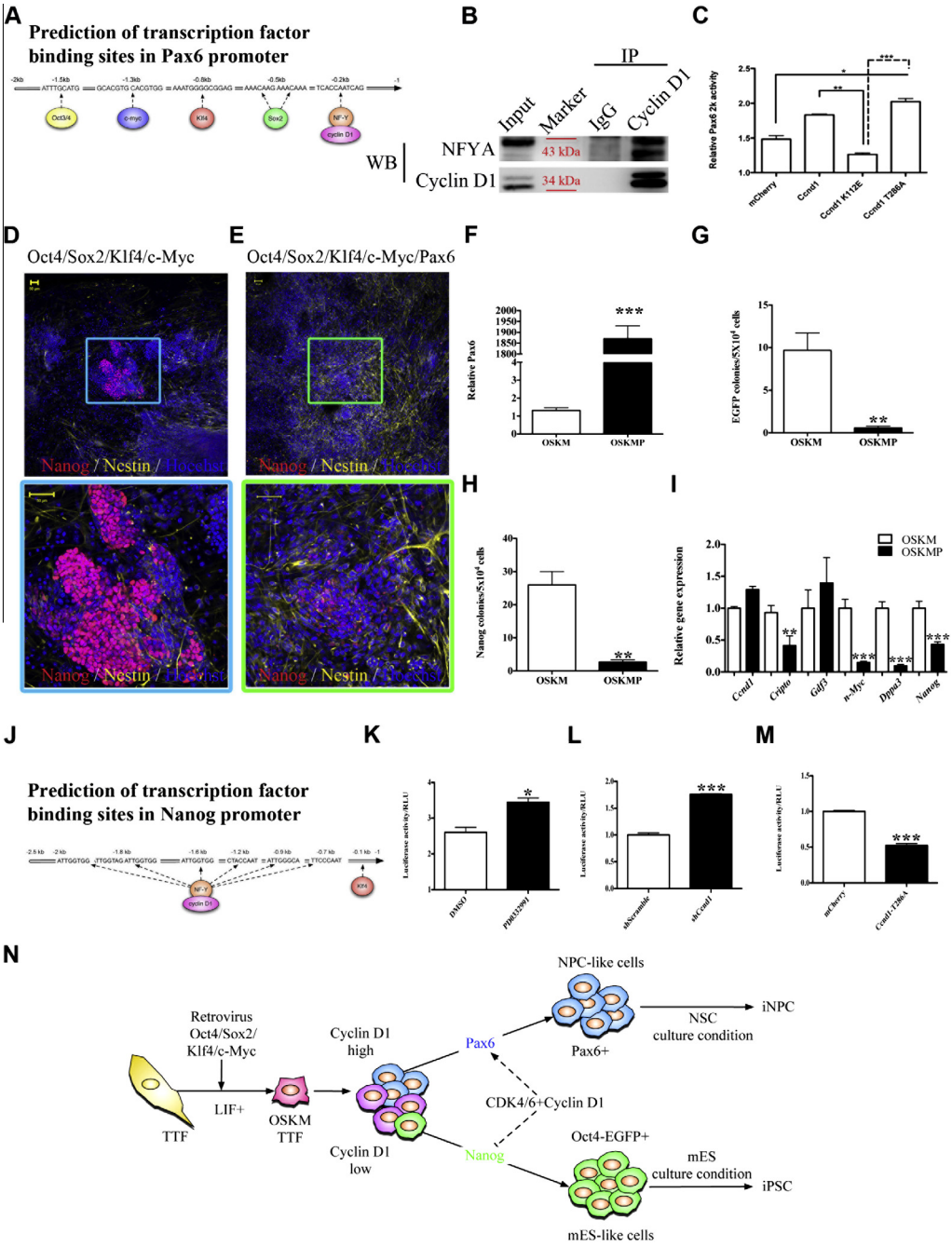

Fig. 5. Cyclin D1 promotes cell reprogramming to neural progenitor commitment by transcriptionally regulating Pax6. (A) Schematic diagram of the 2 kb *Pax6* promoter region. Potential transcription factor binding sites were analyzed with Promo 3.0 software [23]. (B) Total cell extracts (1.5 mg) from EGFP$^-$ cells at passage 5 were immunoprecipitated (IP) with anti-cyclin D1 antibody (2 μg) (lane 4) or a mouse IgG (2 μg) (lane 3). The immunoprecipitates were separated by SDS–polyacrylamide gel electrophoresis, transferred to a PVDF membrane, and probed with anti-cyclin D1 antibody or anti-NF-YA antibody. Cell lysates (20 μg) were also immunoblotted as an input control (lane 1). (C) Sphere cells derived from EGFP$^-$ reprogramming cells at passage 10 were used for the *Pax6* reporter assay. $^*p < 0.05$, $^{**}p < 0.01$, $^{***}p < 0.001$, indicate that the differences between mCherry, *Ccnd1*, *Ccnd1* K112E, and *Ccnd1* T286A treatments were statistically significant. Kruskal–Wallis test was used for determining statistical significance. (D–I) TTF cells were transduced with retroviruses carrying *Oct4*/*Sox2*/*Klf4*/*c-Myc* (OSKM) or *Oct4*/*Sox2*/*Klf4*/*c-Myc*/*Pax6* (OSKMP) and passaged to inactivated MEF feeders in ES culture medium with LIF. After 17 days the reprogramming cells were fixed with 4% PFA and stained with anti-Nestin (yellow) and anti-Nanog (red) antibody (D and E). Cell nuclei were counterstained with Hoechst dye (blue). Scale bar represents 50 μm. (F) Pax6 expression level was quantified with real time qPCR. (G and H) Oct4-EGFP$^+$ or Nanog$^+$ colonies derived from *Oct4*/*Sox2*/*Klf4*/*c-Myc* (OSKM) or *Oct4*/*Sox2*/*Klf4*/*c-Myc*/*Pax6* (OSKMP) were counted under a microscope. (I) The relative gene expression levels of reprogramming cells at Day 17 were analyzed by real-time quantitative PCR for *Ccnd1*, *Cripto*, *Gdf3*, *n-Myc*, *Dppa3*, and *Nanog*. Values shown are mean ± S.E.M., $n = 3$. $^{***}p < 0.001$ and $^{**}p < 0.01$, indicate that the differences between OSKM and OSKMP treatments were statistically significant. Mann–Whitney test was used for determining statistical significance. (J) The 2.5 kb *Nanog* promoter region was analyzed using Promo 3.0 software; the schematic diagram shows potential cyclin D1/NF-Y binding sites. (K–M) For the Nanog reporter assay, the plasmids were transfected with Lipofectamine 3000 and refreshed with ES culture medium after 24-h incubation. At 48 h of transfection, the cells were lysed and the suspension was used in a luciferase activity assay. (K and L) The *Nanog* promoter activity assay in NIH-3T3 cells was performed in the condition of *Ccnd1* knockdown or treatment with the CDK4/6 inhibitor PD0332991. (M) The *Nanog* promoter activity assay in NIH 3T3 cells was performed with overexpression of *Ccnd1* T286A mutant. The value shown is mean ± S.E.M., $n = 3$. $^*p < 0.05$, $^{***}p < 0.001$, indicates that the difference between control and experimental groups was statistically significant. Mann–Whitney test was used for determining statistical significance. (N) Proposed model explains how cyclin D1 acts as a barrier to pluripotent reprogramming by promoting neural progenitor fate commitment. During reprogramming, cyclin D1 can be induced by Yamanaka factors at the initial phase. Sustained production of cyclin D1 can trigger Pax6 expression, which leads to the commitment of reprogramming cells to a neural progenitor fate. In contrast, if cyclin D1 levels are reduced in reprogramming cells, an ES cell-like cell cycle structure can therefore be reestablished, leading to completely pluripotent reprogramming.

tency gene promoters, cyclin D1 can also transcriptionally regulate the level of pluripotency genes. To address this, we analyzed the binding sites of transcriptional factors in the *Nanog* promoter using PROMO 3.0 [23] and found that cyclin D1 can potentially bind, via interacting with NF-Y, to at least 5 sites within the 2.5 kb region of the *Nanog* promoter. A luciferase reporter assay utilizing a *Nanog5P* reporter [28] revealed that *Ccnd1*-knockdown or treatment with the Cdk4/6 inhibitor PD0332991 increased *Nanog5P* reporter activity (Fig. 5J–L). In contrast, overexpression of the stable cyclin D1-T286A mutant suppressed *Nanog* promoter activity (Fig. 5M) [28]. These results suggest that cyclin D1 may act as a transcriptional suppressor of *Nanog*.

The current work demonstrates that cell cycle control is adjusted upon transduction with Yamanaka factors in order to meet the requirements of cell fate commitment either to pluripotent or neural progenitor fate during reprogramming. In addition to the well-established role of cyclin D1 as a G1 phase regulator, our work now suggests a transcriptional role for cyclin D1 in *Pax6* expression, which promotes reprogramming cells towards a neural progenitor fate. We further revealed a requirement for CDK4/6 activity in cyclin D1-regulated *Pax6* expression. As shown in Fig. 5C, overexpression of kinase-dead mutant cyclin D1-K112E suppressed *Pax6* promoter activity. Moreover, treatment of day 3 reprogramming cells with the Cdk4/6 inhibitor PD0332991 also led to a significant reduction of $Pax6^+$ cell clusters and to an increased proportion of Nanog-expressing cells (Supplementary Fig. 9A–E), suggesting that both cyclin D1 and CDK4/6 are required either for NPC maintenance or for suppressing the maintenance of $Nanog^+$ colonies during cell reprogramming (Fig. 4I and J).

A number of recent studies had revealed that pluripotent stem cells exhibit a shortened G1 phase [2,10,20]. During the initial stages of cell differentiation, loss of pluripotency is accompanied by an increase in the length of the G1 phase [20]. Recent works further demonstrated that pluripotent ES cells become more sensitive to differentiation signals in G1 phase, which is the cause of heterogeneity of pluripotent cells [10]. We therefore speculate that, in ES and iPS cells, cyclin D1 is only expressed at a very low level or with a very short half-life in order to ensure the maintenance of a short G1 phase and undifferentiated status. An increase in the level of cyclin D1 can either enhance the sensitivity of pluripotent cells to respond to differentiation stimuli or transcriptionally activate genes such as Pax6 to promote cell differentiation. We propose a model to explain how evaluated levels of cyclin D1 during Yamanaka factor-mediated reprogramming can be linked to neural progenitor fate commitment (Fig. 5J). During the initial reprogramming, the level of cyclin D1 can be up-regulated by Yamanaka factors. However, sustained production of cyclin D1 possibly causes either suppression of pluripotency genes such as *Nanog* or upregulation of *Pax6*, which leads reprogramming cells to become NPCs. If cyclin D1 levels are reduced in reprogramming cells, an ES cell-like cell cycle structure can be reestablished, which will lead to complete pluripotency reprogramming.

Author contributions

C.L.C. and L.J.W. were the main contributors to the experimental work, H.W.H. assisted with RNA seq data analysis, F.P.C. carried out statistical analyses, Y.T.Y., H.L.S., P.C.H. and S.M.H. provided key reagents. C.L.C., L.J.W. and C.N.S. conceived and designed the experiments, C.L.C., L.J.W., Y.T.Y., H.L.S., P.C.H. and C.N.S. analyzed the data, C.L.C. and C.N.S. wrote the paper.

Competing financial interests

The authors declare no competing financial interests.

Acknowledgements

The authors would like to thank Drs. Candy Cho and Winston Chen for critically reviewing the manuscript and acknowledge the flow cytometry facility and the confocal microscope facility at the Genomics Research Center and the Scientific Instrument Center of Academia Sinica for technical assistance. The authors appreciate Dr. Shinya Yamanaka (Center for iPS Cell Research and Application, Kyoto University), Dr. Kevin Eggan (Howard Hughes Medical Institute, Harvard University), and Dr. Austin Cooney (Baylor College of Medicine) for providing the plasmids pMXs-Oct4, pMXs-Sox2, pMXs-Klf4, pMXs-c-Myc, pMXs-Pax6 and the Nanog5p reporter. This work was supported in part by Intramural Grant of Academia Sinica and National Science Council Grants NSC 99-3111-B-001-008, 99-2314-B-001-002-MY3 & 102-2314-B-001-006-MY3 to C.N.S.

Appendix A. Supplementary data

Supplementary data associated with this article can be found, in the online version, at http://dx.doi.org/10.1016/j.febslet.2014.08.039.

References

[1] Hormanseder, E., Tischer, T. and Mayer, T.U. (2013) Modulation of cell cycle control during oocyte-to-embryo transitions. EMBO J. 32, 2191–2203.
[2] Abdelalim, E.M. (2013) Molecular mechanisms controlling the cell cycle in embryonic stem cells. Stem Cell Rev. 9, 764–773.
[3] Calegari, F., Haubensak, W., Haffner, C. and Huttner, W.B. (2005) Selective lengthening of the cell cycle in the neurogenic subpopulation of neural progenitor cells during mouse brain development. J. Neurosci. 25, 6533–6538.
[4] Lange, C., Huttner, W.B. and Calegari, F. (2009) Cdk4/cyclinD1 overexpression in neural stem cells shortens G1, delays neurogenesis, and promotes the generation and expansion of basal progenitors. Cell Stem Cell 5, 320–331.
[5] Roccio, M., Schmitter, D., Knobloch, M., Okawa, Y., Sage, D. and Lutolf, M.P. (2013) Predicting stem cell fate changes by differential cell cycle progression patterns. Development 140, 459–470.
[6] Artegiani, B., Lindemann, D. and Calegari, F. (2011) Overexpression of cdk4 and cyclinD1 triggers greater expansion of neural stem cells in the adult mouse brain. J. Exp. Med. 208, 937–948.
[7] Stead, E., White, J., Faast, R., Conn, S., Goldstone, S., Rathjen, J., Dhingra, U., Rathjen, P., Walker, D. and Dalton, S. (2002) Pluripotent cell division cycles are driven by ectopic Cdk2, cyclin A/E and E2F activities. Oncogene 21, 8320–8333.
[8] White, J. and Dalton, S. (2005) Cell cycle control of embryonic stem cells. Stem Cell Rev. 1, 131–138.
[9] Kalaszczynska, I., Geng, Y., Iino, T., Mizuno, S., Choi, Y., Kondratiuk, I., Silver, D.P., Wolgemuth, D.J., Akashi, K. and Sicinski, P. (2009) Cyclin A is redundant in fibroblasts but essential in hematopoietic and embryonic stem cells. Cell 138, 352–365.
[10] Pauklin, S. and Vallier, L. (2013) The cell-cycle state of stem cells determines cell fate propensity. Cell 155, 135–147.
[11] Takahashi, K. and Yamanaka, S. (2006) Induction of pluripotent stem cells from mouse embryonic and adult fibroblast cultures by defined factors. Cell 126, 663–676.
[12] Okita, K., Ichisaka, T. and Yamanaka, S. (2007) Generation of germline-competent induced pluripotent stem cells. Nature 448, 313–317.
[13] Grskovic, M., Javaherian, A., Strulovici, B. and Daley, G.Q. (2011) Induced pluripotent stem cells–opportunities for disease modelling and drug discovery. Nat. Rev. Drug Discov. 10, 915–929.
[14] Szabo, E., Rampalli, S., Risueño, R.M., Schnerch, A., Mitchell, R., Fiebig-Comyn, A., Levadoux-Martin, M. and Bhatia, M. (2010) Direct conversion of human fibroblasts to multilineage blood progenitors. Nature 468, 521–526.
[15] Thier, M., Wörsdörfer, P., Lakes, Y.B., Gorris, R., Herms, S., Opitz, T., Seiferling, D., Quandel, T., Hoffmann, P., Nöthen, M.M., Brüstle, O. and Edenhofer, F. (2012) Direct conversion of fibroblasts into stably expandable neural stem cells. Cell Stem Cell 10, 473–479.
[16] Kim, J., Efe, J.A., Zhu, S., Talantova, M., Yuan, X., Wang, S., Lipton, S.A., Zhang, K. and Ding, S. (2011) Direct reprogramming of mouse fibroblasts to neural progenitors. Proc. Natl. Acad. Sci. U.S.A. 108, 7838–7843.
[17] Ruiz, S., Panopoulos, A.D., Herrerías, A., Bissig, K.-D., Lutz, M., Berggren, W.T., Verma, I.M. and Izpisua Belmonte, J.C. (2011) A high proliferation rate is required for cell reprogramming and maintenance of human embryonic stem cell identity. Curr. Biol. 21, 45–52.
[18] Yoshimizu, T., Sugiyama, N., De Felice, M., Yeom, Y.I., Ohbo, K., Masuko, K., Obinata, M., Abe, K., Schöler, H.R. and Matsui, Y. (1999) Germline-specific

expression of the Oct-4/green fluorescent protein (GFP) transgene in mice. Dev. Growth Differ. 41, 675–684.
[19] Brambrink, T., Foreman, R., Welstead, G.G., Lengner, C.J., Wernig, M., Suh, H. and Jaenisch, R. (2008) Sequential expression of pluripotency markers during direct reprogramming of mouse somatic cells. Cell Stem Cell 2, 151–159.
[20] Coronado, D., Godet, M., Bourillot, P.Y., Tapponnier, Y., Bernat, A., Petit, M., Afanassieff, M., Markossian, S., Malashicheva, A., Iacone, R., Anastassiadis, K. and Savatier, P. (2013) A short G1 phase is an intrinsic determinant of naïve embryonic stem cell pluripotency. Stem Cell Res. 10, 118–131.
[21] Singh, A.M. and Dalton, S. (2009) The cell cycle and Myc intersect with mechanisms that regulate pluripotency and reprogramming. Cell Stem Cell 5, 141–149.
[22] Tsubouchi, T. and Fisher, A. (2012) Reprogramming and the pluripotent stem cell cycle. Curr. Top. Dev. Biol. 104, 223–241.
[23] Messeguer, X., Escudero, R., Farré, D., Núñez, O., Martínez, J. and Albà, M.M. (2002) PROMO. Detection of known transcription regulatory elements using species-tailored searches. Bioinformatics 18, 333–334.
[24] Bienvenu, F., Jirawatnotai, S., Elias, J.E., Meyer, C.A., Mizeracka, K., Marson, A., Frampton, G.M., Cole, M.F., Odom, D.T., Odajima, J., Geng, Y., Zagozdzon, A., Jecrois, P., Young, R.A., Liu, X.S., Cepko, C.L., Gygi, S.P. and Sicinski, P. (2010) Transcriptional role of cyclin D1 in development revealed by a genetic-proteomic screen. Nature 463, 374–378.
[25] Diehl, J.A., Cheng, M., Roussel, M.F. and Sherr, C.J. (1998) Glycogen synthase kinase-3beta regulates cyclin D1 proteolysis and subcellular localization. Genes Dev. 12, 3499–3511.
[26] Landis, M.W., Pawlyk, B.S., Li, T., Sicinski, P. and Hinds, P.W. (2006) Cyclin D1-dependent kinase activity in murine development and mammary tumorigenesis. Cancer Cell 9, 13–22.
[27] Zhang, X., Huang, C.T., Chen, J., Pankratz, M.T., Xi, J., Li, J., Yang, Y., Lavaute, T.M., Li, X.J., Ayala, M., Bondarenko, G.I., Du, Z.W., Jin, Y., Golos, T.G. and Zhang, S.C. (2010) Pax6 is a human neuroectoderm cell fate determinant. Cell Stem Cell 7, 90–100.
[28] Gu, P., LeMenuet, D., Chung, A.C., Mancini, M., Wheeler, D.A. and Cooney, A.J. (2005) Orphan nuclear receptor GCNF is required for the repression of pluripotency genes during retinoic acid-induced embryonic stem cell differentiation. Mol. Cell. Biol. 25, 8507–8519.